π-Donor/Acceptor Effect on Lindqvist Type Polyoxomolibdates Because of Various Multiple-Bonded Nitrogenous Ligands

Desmond Mac-Leod Carey,[†] Alvaro Muñoz-Castro,[†] Carlos J. Bustos,*[,‡] Juan M. Manríquez,[†] and Ramiro Arratia-Pérez*[,§]

Departamento de Química Inorgánica, Facultad de Química, Pontificia Universidad Católica de Chile, Casilla 306, Correo 22, Santiago, Chile, Instituto de Química, Universidad Austral de Chile, Avda Los Robles s/n, Campus Isla Teja, Casilla 567, Valdivia, Chile, and Facultad de Ecología y Recursos Naturales, Universidad Andrés Bello, República 275, Santiago, Chile

Received: April 9, 2007; In Final Form: May 18, 2007

The electronic structures of Lindqvist type functionalized polyoxometalates (POM) ($[Mo_6O_{18}R]^{n-}$ R = O, NO, NAr, NNAr, $NNAr_2$; $n = 2, 3$) have been investigated using density functional methods. We discuss the role of the replacement of terminal oxo ligands by π-donor/acceptor multiple-bonded nitrogenous ligands on the basis of geometrical parameters, charge analyses, reactivity indexes, and vibrational spectra. The calculated reactivity indexes (chemical potential, electronegativity, hardness, and electrophilicity) indicate that the most reactive functionalized POMs are those substituted by π-acceptor ligands. These π-acceptor ligands induce a decrease in the hardness and an increase in the chemical potential and electrophilicity, thus increasing the reactivity. Our calculations are in reasonable agreement with reported experimental data.

I. Introduction

Early transition-metal oxygen cluster anions, or polyoxometalates (POMs), have been widely studied[1,2] because of their unusual structure[3,4] and their technological applications[5−6] with respect to their electrochemical,[7−9] magnetic,[10] antiviral,[11,12] antimicrobial,[12] and antitumor[11,12] properties. Their further use in catalysis, oxidation, and acidic processes has been also documented.[7,9,13] We think that the functionalization by various ligands may provide a way in which these properties can be tuned and modulated. In particular, we are interested in studying the modification of POM oxygen surfaces by the replacement of terminal oxo ligands by multiple-bonded nitrogenous ligands, such as nitrosyl[14−18] NO^+, organo-imido[19−20] ArN^{2-}, organo-diazenido[21] ArN_2^{2+}, organo-hydrazido[22] $Ar_2N_2^{2-}$, and nitrido[22,23] N^{3-} ligands; most of these are related to the Lindqvist type anion $[Mo_6O_{19}]^{2-}$ and have been prepared by direct reaction of the appropriate organic reagent on the {MoO} function.

Although polyoxoanion chemistry is an extremely rich area of experimental research, high-level calculations on polyoxometalates have remained relatively scarce mainly because of the intensive computational demands imposed by the large size of these species. Regardless of this, recently theoretical investigations of several polyoxometalates have become available. However, they are essentially related to the $[M_6O_{19}]^{n-}$ isopolyanions (M = Nb, Ta, Mo, W).[24−36] On the other hand, in literature can be found quite enough information related to the experimental functionalization of POMs with Lindqvist type structure,[14−23] but only few theoretical studies that involve the functionalization of the $[Mo_6O_{19}]^{2-}$ anion with several arylimido ligands have been recently reported.[37,38] However, no other types of functionalized POMs have been theoretically explored yet.

Our interests on these systems are as follows: (a) How does the functionalization perturb the geometrical parameters of the Mo_6 cage? (b) What is the influence of π-donor/acceptor character of the ligands on the polyoxometalate electronic structure? (c) What is the influence of π-donor/acceptor character of the ligands on the polyoxometalate on their vibrational spectra?.

In this article, we report the electronic structure, geometrical parameters, reactivity indexes, and the calculated vibrational structure of several $[Mo_6O_{19}]^{2-}$ functionalized derivatives obtained by density functional theory (DFT). Our calculated values are in good agreement with available reported experimental results. We hope that the results obtained here will provide helpful guidelines for future synthetic strategies.

II. Computational Details

All density functional calculations reported here were performed with the Amsterdam Density Functional package, ADF 2005.[39] All the cluster structures were fully optimized via analytical energy gradient techniques employing the local density approximation (LDA)[40] and the generalized gradient approximation (GGA) method using Vosko et al.'s local exchange correlations[41] with nonlocal exchange corrections by Becke[42] and nonlocal electronic correlations by Perdew.[43] We used uncontracted type IV basis set using triple-ξ accuracy sets of Slater type orbitals[44] (STO) with a single polarization function added for the main group elements (2p on H and 3d on C). Frozen core approximation[45] was applied to the inner orbitals of the constituent atoms: the C, N, O core up to 1s and Mo up to 3d. The functional and basis set choices were based on the results of tests performed on several $[MoO_4]$ and $[Mo_2O_7]$ species.[46−48]

For the geometry optimizations, we constrained the symmetry as O_h for $[Mo_6O_{19}]^{2-}$, C_{4v} for $[Mo_6O_{18}(NO)]^{3-}$, C_{2v} for

* To whom correspondence should be addressed. Fax: +56 63 221769; e-mail: cbustos@uach.cl (C.J.B.). Fax: +5626618269; e-mail: rarratia@unab.cl (R.A.-P.).

[†] Pontificia Universidad Católica de Chile.

[‡] Universidad Austral de Chile.

[§] Universidad Andrés Bello.

10.1021/jp0727594 CCC: $37.00
Published on Web 06/27/2007

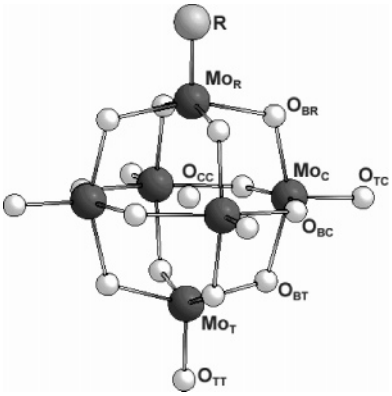

Figure 1. Structural and atom-labeling scheme for $[Mo_6O_{18}R]^{n-}$ anions (R = O, NO, NAr, NNAr, $NNAr_2$; n = 2, 3).

SCHEME 1: Functionalizated Lindqvist Type Polyoxomolibdates Assorted by Its π-Donor/Acceptor Character

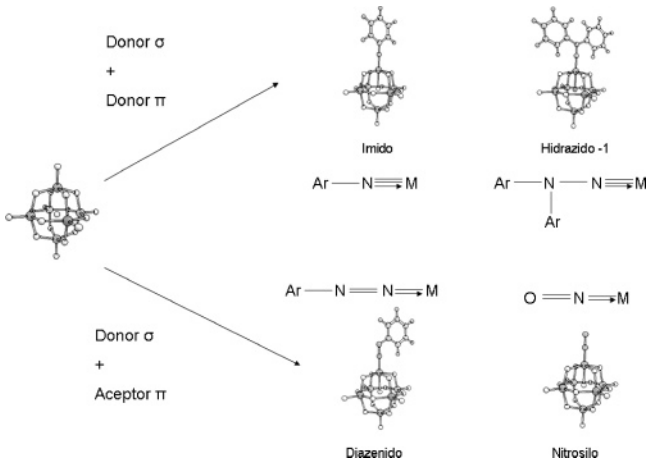

$[Mo_6O_{18}(NNAr_2)]^{2-}$ and $[Mo_6O_{18}(NAr)]^{2-}$, and C_s for $[Mo_6O_{18}(NNAr)]^{3-}$. The choices for these systems were made on the basis of the structural parameters obtained by X-ray diffraction studies.[16,22,49−52]

The vibrational frequency calculations were performed for each cluster at the optimized geometries by determining the second derivatives of the total energy with respect to the internal coordinates as it is implemented in the ADF code.[53−55]

III. Results and Discussion

Here, we report the structural, vibrational, and electronic differences induced by different nitrogenous ligands in several $[Mo_6O_{18}R]^{n-}$ Lindqvist type polyoxometalates. A bonna fide classification suggests that these ligands can be divided into two groups: first, the ones that have a σ- and π-donor character as imido and hydrazido ligands resulting as $[Mo_6O_{18}(NAr)]^{2-}$ and $[Mo_6O_{18}(NNAr_2)]^{2-}$, respectively; second, the ones that have a σ- donor and π-acceptor character as nitrosyl and diazenido ligands resulting as $[Mo_6O_{18}(NO)]^{3-}$ and $[Mo_6O_{18}(NNAr)]^{3-}$, respectively, as depicted in Scheme 1.

Molecular Structure. The calculated and experimental selected distances are given in Table 1, and a structural scheme showing atom labels is presented in Figure 1. All the compounds are isomorphous considering the structural characteristics of the $[Mo_6O_{18}R]^{n-}$ cage. The calculated parameters are in good agreement with the experimental data, as indicated in Table 1. As we expected, as a consequence of the functionalization, the $[Mo_6O_{19}]^{2-}$ cage is distorted by the replacement of the oxo ligand by a nitrogenous ligand, as indicated by the X-ray

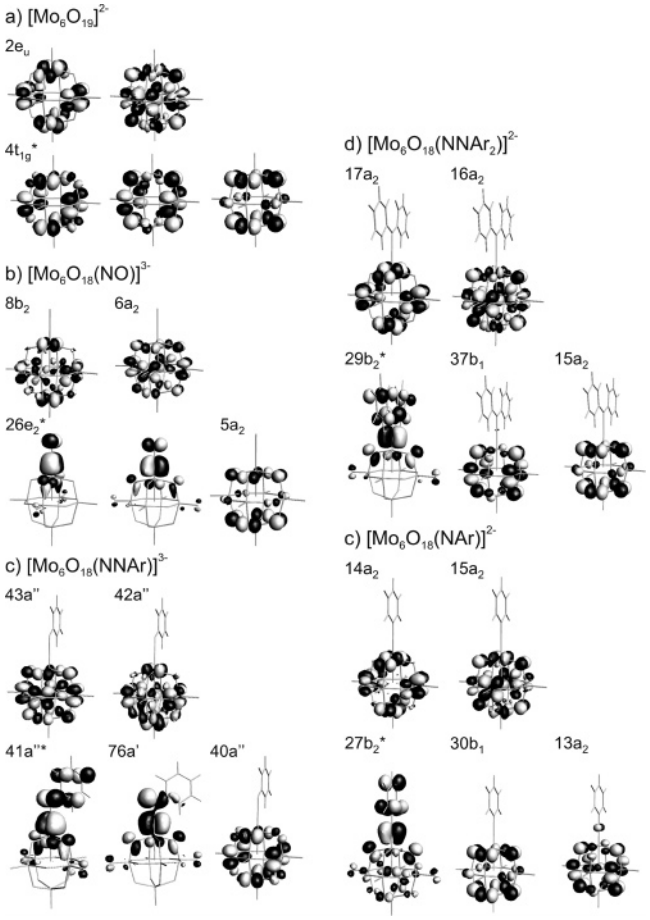

Figure 2. Frontier orbitals spatial representations.

parameters. The Mo_R-O_{CC} distance between the functionalized Mo center and the central oxygen atom is significantly shorter than the $[Mo_6O_{19}]^{2-}$ cage, and consequently the Mo_T-O_{CC} distances between the Mo center opposite to the functionalized Mo center and the central oxygen atom are significantly longer than its analogous $[Mo_6O_{19}]^{2-}$ cage. This general effect has a differentiated influence on the Mo_R-Mo_T distance depending on the π-type character of the ligand. That is, those with π-donor ones do not induce significant changes, but those with π-acceptor character produce a shortening in the Mo_R-Mo_T distance, however, the terminal Mo_C-O_{TC} distances are not significantly changed.

The $Mo_C-Mo_{C'}$ and $Mo_C-Mo_{C''}$ distances (contiguous and opposite equatorial Mo's) are larger than those seen in the unfunctionalized analogous one, which is owed just to an arrangement in the $[Mo_6O_{18}R]^{n-}$ cage. The symmetry reduction from O_h to C_{4v}, C_{2v}, and C_s arises when the oxo ligand is replaced in the $[Mo_6O_{19}]^{2-}$ cage, without affecting the lengths of the $Mo-O_{TC}$ distances significantly, as can be appreciated from Table 1.

A close relationship between the character of the ligands and the distortion of the cage can be found through the sum of the distances Mo_r-Mo_t plus $Mo_c-Mo_{c''}$. This will show us an estimation about the cage area. Comparing this value based on the result of the $[Mo_6O_{19}]^{2-}$ with the functionalizated POMs, we found that the area of the π-donor ligands increases by about 1.0% and that of the π-acceptor ligands decreases by about 0.4%. These small changes in the area of the cage are attributed to the increase or decrease of the charge density in the POM cage, respectively. The ligand π-donor character has a major effect on the length of the $Mo_C-Mo_{C''}$, distance; it increases

TABLE 1: Selected Distances (in pm)

	$[Mo_6O_{19}]^{2-}$		$[Mo_6O_{18}NAr]^{2-}$		$[Mo_6O_{18}NNArAr]^{2-}$		$[Mo_6O_{18}NNAr]^{3-}$		$[Mo_6O_{18}NO]^{3-}$	
	calcd	exptl[a]	calcd	exptl[b]	calcd	exptl[c]	calcd	exptl[d]	calcd	exptl[e]
Mo_R-O_{CC}	235.3	231.9	223.0	224.2	216.2	216.1	218.7	215.0	218.8	227.5
Mo_T-O_{CC}	235.3	231.9	248.6	233.7	253.9	238.6	244.0		243.2	
Mo_C-O_{CC}	235.3	231.9	239.6	231.8	240.5	231.1	237.2	235.0	237.8	2326
Mo_T-Mo_R	470.5		471.7	475.6	470.1	454.7	462.7		462.0	455.1
$Mo_C-Mo_{C'}$	470.5		338.9		339.7	331.0	335.4		336.3	331.2
$Mo_C-Mo_{C''}$	332.7	327.4	479.3		480.4	468.2	474.2		475.6	465.2
Mo_R-O_{BR}	194.2	192.8	199.0	193.0	200.0	195.9	199.7	191.2	200.7	195.2

[a] Reference 21. [b] Reference 19. [c] References 49, 50. [d] Reference 21. [e] Reference 15.

by 5 pm more than the π-acceptor ligands. The effect of the ligand π-acceptor character influences mainly the length of the Mo_r-Mo_t distance, thus reducing it in about 10 pm. In both cases, the O_{CC} atom brings the Mo_R atom closer by about 12 to 18 pm compared against the unsubstituted cage.

Electronic Structure. Some molecular orbital (MO) analyses for the $[M_6O_{19}]^{2-}$ (M = W, Cr, Mo, Nb, Ta) Lindqvist POMs have been presented in early publications.[56−58] However, here we discuss the changes produced by the ligand functionalization over the well-known frontier orbitals $6t_{2g}$ (lowest unoccupied molecular orbital (LUMO) + 1), $2e_u$ (LUMO), $4t_{1g}$ (highest occupied molecular orbital (HOMO)), and $11t_{1u}$ (HOMO − 1) in $[Mo_6O_{19}]^{2-}$. The HOMO (t_{1g}) and LUMO (e_u) of unsubstituted $[Mo_6O_{19}]^{2-}$ cage are shown in Figure 2. Here, we also depict their corresponding orbitals arising from the lowering in symmetry of the functionalized analogous. In the Supporting Information, we give the percent compositions of the functionalized frontier orbitals depicted in Figure 2 and an MO diagram with the orbital correlation and all the isosurface figures for the frontier orbitals.

The LUMO + 1 triple degenerated ($6t_{2g}$) level in $[Mo_6O_{19}]^{2-}$ comprises three orbitals, and each one is constituted by two of the six metal centers (∼67%) in the same axis and by the eight neighbor-bridging oxygen atoms (∼32%) related to those metal centers. This fashion repeats over the three axes, involving the 6 metal centers and the 12 O_b atoms considering the triple degeneracy. In the functionalized POM cages, it can be seen that the LUMO + 1 ($6t_{2g}$) orbital remains unaltered in all the cases, except for the $28b_2$ orbital in the substituted imido POM, because there is a significant electronic density contribution along the *z*-axis introduced by the ligand.

The LUMO is particularly important as it is the acceptor of the additional electrons in the reduced species. In the $[Mo_6O_{19}]^{2-}$ cage, this corresponds to the $2e_u$ level (Figure 2) and is characterized by the participation of the molybdenum metal atoms (∼55%) and the bridging oxygen atoms (∼43%).

A three-dimensional spatial representation of the two degenerated orbitals of the $2e_u$ level is given in Figure 2a. One of these is conformed by four of the six metal centers and eight of the bridging oxygen atoms, and the other implies the participation of the 6 metal centers and the 12 bridging oxygens and can also be described in terms of three planar $[Mo_4O_4]$ rings that correspond to the closed loops proposed by Nomiya and Miwa.[59]

The π-donor ligands do not affect the composition of the LUMO orbital by replacing the oxo ligand; this can be noticed from the spatial representations of the molecular orbitals (Figure 2d, 2e). The π-acceptor ligands affect one of the two $2e_u$ MOs, being $42a''$ in the diazenido POM and $8b_2$ in the nitrosyl POM, which shows a decreasing density in the functionalized sector over the orbital composition and an increasing density in the terminal sector; this is the opposite sector to the functionalized one. These can be noticed from the spatial representations of the corresponding orbital, see Figure 2b, 2c. The triple-degenerated HOMO ($4t_{1g}$) is mainly localized in the nonbonding lone pairs of the O_B atoms in the $[Mo_6O_{19}]^{2-}$ cage.

The π-acceptor ligands affect those orbitals that transform as e symmetry in the nitrosyl derivative and those that correlate with $a'' + a'$ symmetry in diazenido. Thus, they show a clear effect that slides the electronic density from the cage toward the nitrogenous ligand and its Mo_R surroundings, leaving the rest of the cage almost without any electronic density.

Moreover, the π-donor ligands only affect notoriously those MOs with b_2 symmetry in the hidrazido and imido derivatives, thus producing the same effect that slides the electronic density like in the acceptor ones. The other orbital with b_1 symmetry remains almost unaffected like those with a_2 symmetry.

The triply degenerated HOMO − 1 ($11t_{1u}$), in $[Mo_6O_{19}]^{2-}$, is delocalized over the central (∼44%), bridging (∼41%), and terminal (∼15%) oxygen atoms.

For the functionalized cages, they have a differentiated effect depending on the π-type ligand. In the π-donor ligands, the orbitals with b_1 and a_1 symmetry slightly increase their density by including the ligand contribution; however, in those with b_2 symmetry, almost all the electronic density of the O_{CC} atom is transferred to the O_{BT} atoms. In the π-acceptor derivatives, the $74a'$ and $26a_1$ orbitals slightly increase their density by including the ligand contribution like the b_1 and a_1 in the π donors. In the 26e, $75a'$, and $40a''$ orbitals, the electronic density of the O_{CC} atom is transferred mainly to the O_B atoms.

Vibrational Properties. The vibrational patterns located at low-wavenumber region of the IR spectra ($\nu < 1000$ cm^{-1}) are very useful for the characterization and identification of various Lindqvist type polyoxometalates.

As expected, the functionalization produces a distortion in the cage geometry, in addition to the reduction of symmetry, which modifies the cage vibrational pattern. We provide in Table 2 the magnitude, wavenumbers, and symmetry of the Mo−O−Mo and $Mo-O_T$ stretching modes for each substituted POM.

The vibrational pattern corresponding to the Mo−O−Mo stretching modes, split into three vibrational peaks corresponding to the ν(Mo−O_{BR}−Mo), ν(Mo−O_{BC}−Mo), and ν(Mo−O_{BT}−Mo) modes, is a consequence of the functionalization. Also, the $Mo-O_T$ stretching mode splits into two vibrational peaks corresponding to the ν(Mo−O_{TC}) and ν(Mo−O_{TT}) modes (see Table 2). Thus, the calculated frequencies are in good agreement with experimental results.

Charge Analyses and Reactivity Indexes. The variation of the electronic charge in the cage atoms was studied by three methods. These are the charge definitions by Mulliken, Hirshfeld, and Voronoi (VDD).[60] The three methods describe the same tendency, showing that the π-acceptor ligands increase the charge on the Mo_R atom compared with the unsubstituted POM and that the π-donor ligands produce a charge decrease on the Mo_R atom. Also, the charge density for π-donor and π-acceptor ligands increases the O_{CC} charge.

TABLE 2: Stretching Vibrational Frequencies

assignment	wavenumber (cm^{-1}) experimental	calculated	
T_{1u}: Mo−O−Mo	796[b]	737 (741)	$[Mo_6O_{19}]^{2-}$
T_{1u}: Mo=O	958	865 (865)	
E_1: Mo−O_{BC}−Mo		717 (680)	$[Mo_6O_{18}(NO)]^{3-}$
E_2: Mo−O_{BC}−Mo	795[c]	717 (680)	
A_1: Mo−O_{BR}−Mo		718 (293)	
A_1: Mo−O_{BT}−Mo		731 (425)	
E_1: Mo=O_{TC}	965	902 (279)	
E_2: Mo=O_{TC}		902 (279)	
A_1: Mo=O_{TT}	940	907 (112)	
A_1: Mo=O		915 (6)	
A′: Mo−O_{BR}−Mo	762[d]	755 (369)	$[Mo_6O_{18}(NNPh)]^{3-}$
A′: Mo−O−Mo		787 (796)	
A″: Mo−O_{BC}−Mo	786	787 (700)	
A′: Mo−O_{BT}−Mo		805 (426)	
A′: Mo=O_{TC}	962	983 (77)	
A′: Mo=O_{TC}		988 (37)	
A′: Mo=O_{TT}		1001 (86)	
A′: Mo=O_{TC}		1008 (90)	
A_1: Mo−O_{BR}−Mo		707 (756)	$[Mo_6O_{18}(NNPhPh)]^{2-}$
B_1: Mo−O_{BC}−Mo		713 (711)	
B_2: Mo−O_{BC}−Mo	780[e]	714 (752)	
A_1: Mo−O_{BT}−Mo		725 (402)	
A_1: Mo=O_{TC}		901 (0.3)	
A_1: Mo=O	943	906 (37)	
A_1: Mo=O		911 (25)	
B_2: Mo−O_{BC}−Mo		733 (616)	$[Mo_6O_{18}(NPh)]^{2-}$
A_1: Mo−O_{BR}−Mo		733 (849)	
B_1: Mo−O_{BC}−Mo		735 (754)	
A_1: Mo−O_{BC}−Mo	795[f]	737 (105)	
A_1: Mo−O_{BT}−Mo		743 (360)	
A_1: Mo=O_{TC}	955	930 (0.1)	
A_1: Mo=O		935 (67)	
A_1: Mo=O		941 (11)	

[a] Band intensities (km/mol) is given between parentheses. [b] Reference 21. [c] Reference 15. [d] Reference 21. [e] Reference 22, on basis of $[Mo_6O_{18}(NNMePh)]^{2-}$. [f] Reference 19.

TABLE 3: Reactivity Indexes (eV)

electrophilicity ω	hardness η	chemical potential $\mu = -\chi$	
0.2563	1.2550	0.8020	$[Mo_6O_{19}]^{2-}$
19.2162	0.6185	4.8755	$[Mo_6O_{18}(NO)]^{3-}$
21.5701	0.4740	4.5220	$[Mo_6O_{18}(NNPh)]^{3-}$
0.6010	0.8690	1.0220	$[Mo_6O_{18}(NNPhPh)]^{2-}$
0.3707	1.1085	0.9065	$[Mo_6O_{18}(NPh)]^{2-}$

The calculated reactivity indexes (chemical potential, electronegativity, hardness, and electrophilicity) are shown in Table 3. It can be seen from this table that the most reactive functionalized POMs are those substituted by π-acceptor ligands. It can be deduced that the replacement of the O atom in the $[Mo_6O_{19}]^{2-}$ cage produces a decrease in the hardness, thus increasing their reactivity. This reactivity effect is greater in those POMs functionalized by π-acceptor ligands; see Table 3.

IV. Conclusions

The replacement of terminal oxo ligand in the $[Mo_6O_{19}]^{2-}$ cage by various multiple-bonded nitrogenous ligands has a marked influence on the cage geometrical parameters. That is, π-donor ligands expand the cage, and those with π-acceptor character produce a cage compression. Also as discussed, the functionalization produces a distortion in the cage geometry, thus modifying the cage vibrational pattern corresponding to the Mo−O−Mo stretching modes, which are split into three vibrational peaks, and the Mo−O_T stretching mode, which is split into two vibrational peaks, as a consequence of the functionalization. The calculated frequencies are in good agreement with experimental results.

The calculated reactivity indexes (chemical potential, electronegativity, hardness, and electrophilicity) indicate that the most reactive functionalized POMs are those substituted by π-acceptor ligands. These π-acceptor ligands induce a decrease in the hardness and an increase in the chemical potential and electrophilicity, thus increasing the reactivity. This information is quite useful for planning supramolecular syntheses because the reactivity can be modulated or tuned by the inclusion of different types of ligands.

Acknowledgment. D.M.C. is grateful for grant "Apoyo de Tesis Doctoral" CONICYT project N° 23070215. C.B. is grateful for the investigation projects FONDECYT Grants N° 1000437, PICS CNRS/CONICYT Grant N° 929, and DID-UACh Grant N° S-2006-45. R.A.P. is grateful for support from Fondecyt N° 1070345, UNAB-DI 42-06/R, Millennium Nucleus for Applied Quantum Mechanics and Computational Chemistry P02-004-F, and MECESUP FSM0605. J.M.M. is grateful for FONDECYT grant N° 1060589.

Supporting Information Available: Energy level diagram, MO diagrams, Porcentual orbital diagram, charge figures, and table of charge analysis data. This material is available free of charge via the Internet at http://pubs.acs.org.

References and Notes

(1) Pope, M. T. *Heteropoly and Isopoly Oxometalates*; Springer: Berlin, 1983.
(2) Baker, L. C. W.; Glick, D. C. *Chem. Rev.* **1998**, *98*, 3.
(3) Pope, M. T.; Muller, A. *Angew. Chem., Int. Ed. Engl.* **1991**, *30*, 34.
(4) Jeannin, Y. P. *Chem. Rev.* **1998**, *98*, 51.
(5) Katsoulis, D. E. *Chem. Rev.* **1998**, *98*, 359.
(6) Coronado, E.; Gómez-García, C. J. *Chem. Rev.* **1998**, *98*, 273.
(7) Sadakane, M.; Steckhan, E. *Chem. Rev.* **1998**, *98*, 219.
(8) Weinstock, I. A. *Chem. Rev.* **1998**, *98*, 113.
(9) Kozhevnikov, I. V. *Chem. Rev.* **1998**, *98*, 171.
(10) Müller, A.; Peters, F.; Pope, M. T.; Gatteschi, D. *Chem. Rev.* **1998**, *98*, 239.
(11) Rhule, J. T.; Hill, C. L.; Judd, D. A. *Chem. Rev.* **1998**, *98*, 327.
(12) Hasenknopf, B. *Front. Biosci.* **2005**, *10*, 275.
(13) Mizuno, N.; Misono, M. *Chem. Rev.* **1998**, *98*, 199.
(14) Proust, A.; Thouvenot, R.; Robert, F.; Gouzerh, P. *Inorg. Chem.* **1993**, *32*, 5299.
(15) Proust, A.; Thouvenot, R.; Roh, S. G.; Yoo, J. K.; Gouzerh, P. *Inorg. Chem.* **1995**, *34*, 4106.
(16) Gouzerh, P.; Jeannin, Y.; Proust, A.; Robert, F. *Angew. Chem., Int. Ed. Engl.* **1989**, *28*, 1363; **1989**, *101*, 1377.
(17) Proust, A.; Gouzerh, P.; Robert, F. *Inorg. Chem.* **1993**, *32*, 5291.
(18) Proust, A.; Fournier, M.; Thouvenot, R.; Gouzerh, P. *Inorg. Chim. Acta* **1994**, *215*, 61.
(19) Proust, A.; Thouvenot, R.; Chaussade, M.; Robert, F.; Gouzerh, P. *Inorg. Chim. Acta* **1994**, *224*, 81.
(20) Strong, J. B.; Yap, G. P. A.; Ostrander, R.; Liable-Sands, L.; Rheingold, A. L.; Thouvenot, R.; Gouzerh, P.; Maatta, E. A. *J. Am. Chem. Soc.* **2000**, *122*, 639.
(21) Bustos, C.; Hasenknopf, B.; Thouvenot, R.; Vaissermann, J.; Proust, A.; Gouzerh, P. *Eur. J. Inorg. Chem.* **2003**, 2757.
(22) Kang, H.; Zubieta, J. *J. Chem. Soc., Chem. Commun.* **1988**, 1192.
(23) Kwen, H.; Tomlinson, S.; Maatta, E. A.; Dablemont, C.; Thouvenot, R.; Proust, A.; Gouzerh, P. *Chem. Commun.* **2002**, 2970.
(24) Li, J. *J. Cluster Sci.* **2002**, *13*, 137.
(25) Bridgeman, A. J.; Cavigliasso, G. *J. Phys. Chem. A* **2003**, *107*, 4568.
(26) Bridgeman, A. J.; Cavigliasso, G. *Inorg. Chem.* **2002**, *41*, 1761.
(27) Yang, X.; Waters, T.; Wang, X. B.; O'Hair, R. A. J.; Wedd, A. G.; Li, J.; Dixon, D. A.; Wang, L. S. *J. Phys. Chem. A* **2004**, *108*, 10089.
(28) Rohmer, R. M.; Bénard, M.; Blaudeau, J. P.; Maestre, J. M.; Poblet, J. P. *Coord. Chem. Rev.* **1998**, *178−180*, 1019.

(29) Masure, D.; Chaquin, P.; Louis, C.; Che, M.; Fournier, M. *J. Catal.* **1989**, *119*, 415.
(30) Calhorda, M. J. *J. Organomet. Chem.* **1994**, *475*, 149.
(31) Dolbecq, A.; Guirauden, A.; Fourmigué, M.; Boubekeur, K.; Batail, P.; Rohmer, M. M.; Bénard, M.; Coulon, C.; Sallé, M.; Blanchard, P. *J. Chem. Soc., Dalton Trans.* **1999**, 1241.
(32) Bridgeman, A. J.; Cavigliasso, G. J. *J. Chem. Soc., Dalton Trans.* **2002**, 2244.
(33) Bridgeman, A. J.; Cavigliasso, G. J. *Inorg. Chem.* **2002**, *41*, 3500.
(34) Bridgeman, A. J.; Cavigliasso, G. J. *J. Phys. Chem. A* **2002**, *106*, 6114.
(35) Bridgeman, A. J.; Cavigliasso, G. *Polyhedron* **2002**, *21*, 2201.
(36) Kempf, J. Y.; Rohmer, M. M.; Poblet, J. M.; Bo, C.; Bénard, M. *J. Am. Chem. Soc.* **1992**, *114*, 1136.
(37) Yan, L.; Yang, G.; Guan, W.; Su, Z.; Wang, R. *J. Phys. Chem. B* **2005**, *109*, 22332.
(38) Yan, L. K.; Su, Z.-M.; Guan, W.; Zhang, M. *J. Phys. Chem. B* **2004**, *108*, 17337.
(39) ADF2005.01: te Velde, G.; Baerends, E. J. *J. Comput. Phys.* **1992**, *99*, 84.
(40) Kohn, W.; Sham, L. J. *Phys. Rev.* **1965**, *140*, A1133.
(41) Vosko, S. H.; Wilk, L.; Nusair, M. *Can. J. Phys.* **1990**, *58*, 1200.
(42) Becke, A. D. *Phys. Rev. A* **1988**, *38*, 3098.
(43) Perdew, J. P. *Phys. Rev. B* **1986**, *33*, 8822.
(44) Snijder, J. G.; Baerends, E. J.; Vernooijs, P. *At. Nucl. Data Tables* **1982**, *26*, 483.
(45) Baerend, E. J.; Ellis, D. E.; Ros, P. *Chem. Phys.* **1973**, *2*, 41.
(46) Bridgeman, A. J.; Cavigliasso, G. *Polyhedron* **2001**, *20*, 2269.
(47) Bridgeman, A. J.; Cavigliasso, G. *J. Phys. Chem. A* **2001**, *105*, 7111.
(48) Bridgeman, A. J.; Cavigliasso, G. *J. Phys. Chem. A* **2003**, *107*, 4568.
(49) Allcock, H. R.; Bissell, E. C.; Shawl, E. T. *Inorg. Chem.* **1973**, *12*, 2963.
(50) Allcock, H. R.; Bissell, E. C.; Shawl, E. T. *J. Am. Chem. Soc.* **1972**, *94*, 8603.
(51) Chen, T. Ch.; Zubieta, J. *Polyhedron* **1986**, *5*, 1655.
(52) Proust, A.; Thouvenot, R.; Chaussade, M.; Robert, F.; Gouzerh, P. *Inorg. Chim. Acta* **1994**, *224*, 81.
(53) Berces, A.; Dickson, R. M.; Fan, L.; Jacobsen, H.; Swerhone, D.; Ziegler, T. *Comput. Phys. Commun.* **1997**, *100*, 247.
(54) Jacobsen, H.; Berces, A.; Swerhone, D.; Ziegler, T. *Comput. Phys. Commun.* **1997**, *100*, 263.
(55) Wolff, S. K. *Int. J. Quantum Chem.* **2005**, *104*, 645.
(56) Bridgeman, A. J.; Cavigliasso, G. *Inorg. Chem.* **2002**, *41*, 1761.
(57) Yang, X.; Waters, T.; Wang, X. B.; O'Hair, R. A. J.; Wedd, A. G.; Li, J.; Dixon, D. A.; Wang, L. S. *J. Phys. Chem. A* **2004**, *108*, 10089.
(58) Li, J. *J. Cluster Sci.* **2002**, *13*, 137.
(59) Nomiya, K.; Miwa, M. *Polyhedron* **1984**, *3*, 341.
(60) Fonseca, C.; Handgraaf, J.-W.; Baerends, E. J.; Bickelhaupt, F. M. *J. Comput. Chem.* **2004**, *25*, 189.